Acta Geotechnica (2022) 17:4473–4483
https://doi.org/10.1007/s11440-022-01504-w

RESEARCH PAPER

Effects of free iron oxide on thermal properties of undisturbed lateritic clay subjected to drying and wetting

Yunshan Xu[1,2,3] · De'an Sun[3] · Zhaotian Zeng[4]

Received: 23 September 2021 / Accepted: 18 February 2022 / Published online: 26 March 2022
© The Author(s), under exclusive licence to Springer-Verlag GmbH Germany, part of Springer Nature 2022

Abstract
Knowledge of soil thermal properties is necessary for the thermal evaluation and design in geotechnical engineering. In this study, the soil thermal properties of undisturbed lateritic clay with and without free iron oxides were measured during drying and wetting. Furthermore, mercury intrusion porosimetry and scanning electron microscopy tests were conducted on specimens to investigate how the free iron oxides affect the soil microstructure. Test results revealed that the thermal conductivity and diffusivity of the undisturbed lateritic clay with the free iron oxides removed (i.e., treated specimens) were higher than those with the free iron oxides (i.e., untreated specimens). The hysteresis effect on the soil thermal conductivity had reduced after removing the free iron oxides. Investigations showed that the microstructure of the treated specimens was denser, and the debris and granular units considerably increased compared with those of untreated specimens. The number and size of soil pores in the treated specimens was lower and smaller than those of untreated specimens. The difference in thermal conductivity and diffusivity between the treated and untreated specimens was mainly attributed to the different extent or quality of connections between neighbouring soil particles that affected the conductive heat transfer in specimens. After removing the free iron oxides, the connection and inclusion of the stable aggregates were destroyed; thus, the relatively large soil pores disappeared. The further dispersion of the soil particles forming the aggregates filled the relatively small pores in specimens, which increased the heat transfer path between neighbouring soil particles.

Keywords Free iron oxide · Lateritic clay · Microstructure · Thermal property · Undisturbed specimen

1 Introduction

Lateritic clay is a high-plasticity soil formed by weathering, laterization, and hydration of different types of parent rocks in a warm and humid climate. It is widely developed in South China, southwestern Japan, South America, eastern as well as southern Africa, and Thailand [25, 37]. The weathering and laterization environments of lateritic clay in different regions are different, which cause the diversification in soil-forming products. Thus, the geological characteristics and engineering properties of lateritic clay have certain regional differences. The lateritic clay usually undergoes three stages of formation process: decalcified magnesium-rich silicon and aluminum, iron-rich manganese, and desilication-rich aluminum. The characteristic products represented by each stage are clay minerals, iron-manganese oxides, and gibbsite, respectively. Accurately characterizing the mineral composition of lateritic clay is

✉ Yunshan Xu
xuyunshan@shu.edu.cn

✉ De'an Sun
sundean@shu.edu.cn

1 School of Civil Engineering, Fujian University of Technology, 33 Xuefu South Road, Fuzhou 350118, People's Republic of China

2 Key Laboratory of Underground Engineering, Fujian Province University, Fuzhou 350118, People's Republic of China

3 Department of Civil Engineering, Shanghai University, 99 Shangda Road, Shanghai 200444, People's Republic of China

4 Guangxi Key Laboratory of New Energy and Building Energy Saving, Guilin University of Technology, Guilin 541004, People's Republic of China

very important. Most lateritic clays exhibit undesirable physical properties, such as high natural water content, high plasticity, and low compactness. However, they demonstrate excellent mechanical properties, such as high shear strength and low compressibility; therefore, they are widely used as building materials [25, 39]. According to the literature, the special engineering properties of lateritic clay could be attributed to the existence of free iron oxides in different occurrence types, such as the forms of bridge, cladding, and crystalline particles [6, 8, 24, 40]. Moreover, free iron oxides in the soil will be destroyed, denatured, and migrated when the environmental physical and chemical factors change, causing a change in the physical and mechanical properties of lateritic clay. Therefore, the influence of free iron oxides on the engineering properties of lateritic clay is a particularly complex issue, which needs further research.

Numerous studies have been conducted on effects of iron oxides on the hydromechanical and physicochemical properties of tested soils. For instance, studies conducted by Duiker et al. [7] suggested that iron oxides and their hydrates in the soil improved the aggregate stability. Furthermore, Rhoton et al. [22] observed that iron oxides caused the formation of bonds with soil particles in acidic soil environments and an increase in the aggregate stability. Wilsona et al. [29] reported that soil aggregates formed by the iron oxides changed the macrostructure and the buffer performance of the soil. Zhang et al. [40] explored how the physicochemical properties of the soil change when removing free iron oxides. They suggested that the free iron oxide provided structural cementation in the soil, which improved its strength and decreased the shrink–swell capacity. Recently, Niu et al. [18] studied how free iron oxides affect the water retention behavior using selective dissolution techniques. They observed that in the low suction range, the soil–water characteristic curve (SWCC) of undisturbed specimens where the free iron oxides were removed by selected chemical techniques was gentler that that of untreated specimens. However, few studies particularly investigated the effects of free iron oxides on the soil thermal properties on the microscale.

The thermal parameters of soil are crucial in characterizing its ability to conduct or store heat. These include thermal conductivity, thermal diffusivity, and specific heat capacity, which control heat transfer and storage under the ground. Accordingly, numerous studies have been conducted on the soil thermal properties and its influence factors, such as the saturation, dry density, mineral, particle shape, aggregate size, porosity, temperature, pore fluid salinity, aging time and soil microstructure [1, 10, 12–17, 26–28, 31, 32, 34–36, 38, 42]. Understanding the soil thermal properties is important for heat transfer analysis, modeling, and suitable designs in many earth-contact thermal engineering projects, such as artificial ground freezing [9, 41], disposal of high-level radioactive waste [26, 33], thermal remediation of polluted soil [3, 5], exploitation of deep mineral resources [20], heat rejection from buried high-voltage cables [19], geothermal energy extraction [4, 21], and construction of a liner system in a refuse landfill [2, 23]. In these thermal engineering projects, the environmental physical and chemical factors will inevitably change, which will eventually affect the occurrence characteristics of free iron oxides. The potential of the special connection form and soil microstructure formed by the cementation of free iron oxides to affect the soil thermal properties has not attracted research attention. Therefore, much research attention needs to be focused on the effects of free iron oxides on the soil thermal properties.

The areas where the lateritic clay is distributed have a tropical or subtropical and humid climate. The seepage and solar radiation at shallow depths generated by frequent precipitation and the hot sun, respectively, have a prominent influence on the engineering properties of lateritic clay. Under extreme climate, the occurrence characteristics of free iron oxides will inevitably change, which will eventually affect the soil thermal properties. The objective of this study was to characterize the alteration in soil microstructure of undisturbed lateritic clay as well as its microscopic mechanism caused by cementation and evaluate their effects on the thermal properties. The thermal properties of undisturbed specimens were measured using a thermal probe method. The effects of free iron oxides on the soil microstructure evolution were investigated using mercury intrusion porosimetry (MIP) and scanning electron microscopy (SEM) techniques.

2 Materials and methods

2.1 Materials

The lateritic clay used in this study is a typical residual soil formed by carbonate rocks extensively distributed in the Guangxi Autonomous region, China. Soil samples were collected from the campus of the Guangxi Normal University at a depth ranging from 2 to 4 m. Owing to the high dispersion of impregnated iron oxide, the tested lateritic clay is brownish-red. The detailed grain size distribution, physical property indices, chemical composition, and mineralogical composition of the soil samples studied are listed in Tables 1, 2, and 3, respectively. As shown in Table 1, the lateritic clay is a type of soil with high liquid limit and mainly shrinkage. In this study, the lateritic clay contains kaolinite, illite, and goethite, which means that its

Table 1 Physical property indexes of lateritic clay

Specific gravity	Liquid limit (%)	Plastic limit (%)	Shrinkage limit (%)	Volume shrinkage ratio (%)	Shrinkage coefficient	Free swelling ratio (%)	Grain size distribution (%)		
							Sand 2–0.05 mm	Silt 0.05–0.002 mm	Clay < 0.002 mm
2.74	61.8	38.1	27.1	15.51	0.23	25	24.95	29.96	45.09

Table 2 Chemical composition of lateritic clay

Lateritic clay	Relative chemical composition (%)							
	Al_2O_3	Fe_2O_3	SiO_2	CaO	MgO	K_2O	Na_2O	Others
Undisturbed specimen	26.68	7.19	55.81	0.39	0.56	3.10	0.32	5.95
Undisturbed specimen with free iron oxide removed	23.54	0.53	60.35	0.13	0.05	4.21	2.86	8.33

Table 3 Mineralogical composition of lateritic clay

Lateritic clay	Relative mineralogical composition (%)						
	Kaolinite	Illite	Goethite	Feldspar	Brucite	Quartz	Others
Undisturbed specimen	30.7	12.0	8.1	9.9	4.6	34.7	3.1
Undisturbed specimen with free iron oxide removed	28.4	11.5	0.4	10.6	5.1	41.6	2.4

lateritization is in the second stage (i.e., stage of iron-rich manganese).

2.2 Specimen preparation

The undisturbed specimens were prepared for the thermal property, MIP and SEM tests. The undisturbed samples were obtained by excavation, with the sampling depth ranging from 2.0 to 4.0 m. When the excavation reached the target soil depth, the steel rings with an inner height of 5.2 cm and a diameter of 7.0 cm were used to vertically press down into the soil layer for sampling and were sealed with a plastic film. After conducting the measurements, the natural water content and dry density of undisturbed specimen were found to be approximately 27.5% and 1.55 g/cm^3, respectively.

The selective dissolution techniques were adopted for removing free iron oxides in the undisturbed specimens. The traditional permeameter was modified into an infiltration device to selectively dissolve and remove free iron oxides from the undisturbed specimens. According to Wiriyakitnateekul et al. [30] and Jiang and Liu [11], the widely used dithionite–citrate–bicarbonate (DCB) solution was first prepared for standby (Fig. 1a). The free iron oxides in undisturbed specimens were removed using the DCB solution as the osmotic solution with the infiltration device (Fig. 1b). The infiltration process using the DCB solution lasted for 60 days. Then, a continuous infiltration for 30 days was conducted using deionized water as an osmotic solution. According to Zhang et al. [40], the removal rate of free iron oxides from the soil with the selective dissolution technique can exceed 85%. As shown in Tables 2 and 3, the removal rate of free iron oxides in this study exceeded 90%, which can basically ensure the test accuracy considering the influence of free iron oxides on the soil thermal properties (see Sect. 2.3).

Eight undisturbed specimens were prepared for the thermal property, MIP and SEM tests (Table 4). Two undisturbed specimens containing free iron oxides (namely U1 and U2) were prepared for testing their thermal properties and measure repeatability. For comparison, two undisturbed specimens that did not contain free iron oxides (namely QTU1 and QTU2) were prepared for testing their thermal properties. Four more specimens were used for microstructure investigations.

2.3 Soil thermal property test

To more reliably simulate the change in soil moisture under natural conditions, specimens containing different amounts

of water were obtained using the spray method and the air-drying method. During the air-drying process, the undisturbed specimens containing an initial water amount of 27.5% were air-dried at laboratory under a constant temperature set to 20 ± 0.5 °C. According to Xu et al. [37], the holding time was about 20 days to ensure the uniform distribution of moisture within specimens during drying and wetting. In this study, the specimens were sealed immediately with a plastic bag for 25 days to ensure that the moisture in specimens was homogenized after water content of 3% was removed. Subsequently, the soil thermal properties were measured during each stage of drying. During the wetting process, the air-dried specimens were wetted using the spray method. After each spray that contained 3% water, the specimens were wrapped immediately with a sealed bag for 25 days before conducting thermal property tests. The specimen volume changed during the air-drying and wetting processes. Therefore, the vernier caliper was used to continuously measure the specimen volume and calculate the real-time dry density during the test procedures.

The thermal probe method was employed as a transient method to measure the soil thermal properties using a commercially available KD2 Pro thermal analyzer, which comprised a controller and three types of thermal probes (i.e., KS-1, TR-1, and SH-1). Both KS-1 probe and TR-1 probe can only measure the thermal conductivity of soil samples, while TR-1 probe is more suitable for measuring thermal conductivity of rock. The main advantage of SH-1 dual probe is simultaneously measuring thermal conductivity, thermal diffusivity, and volumetric heat capacity. In this study, the SH-1 probe was adopted for conducting thermal property tests. The SH-1 probe can simultaneously measure the soil thermal properties at with accuracies as high as ± 5%, ± 5%, and ± 10% for thermal conductivity, thermal diffusivity, and specific heat capacity, respectively. The ambient temperature of the SH-1 probe is between − 50 °C and 150 °C. During the thermal property tests, the insertion of the SH-1 probe into a soil specimen was first conducted and then the controller of KD2 Pro thermal analyzer was used to start measuring soil thermal properties. By monitoring the temperature variation in the

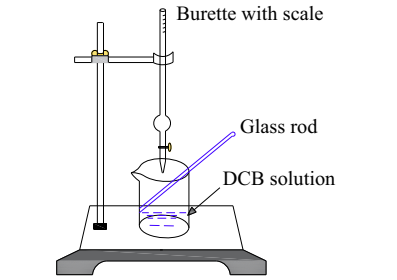

(a) Preparation of dithionite-citrate-bicarbonate (DCB) solution

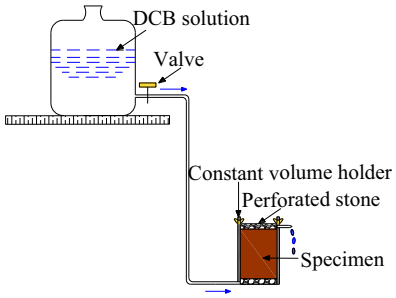

(b) Removal of free iron oxide with DCB solution

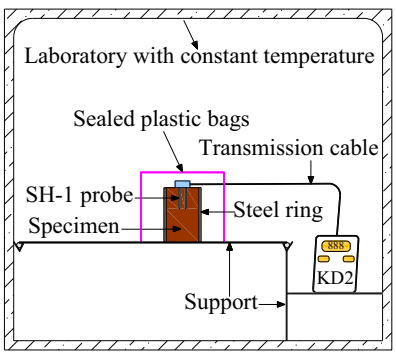

(c) Measurement of thermal properties with KD2 Pro

Fig. 1 Schematic diagram of experimental procedures

Table 4 Samples for thermal property, MIP and SEM tests

Test no	Specimen preparation method	Test type
U1	Undisturbed and subjected to drying-wetting	Thermal property test
U2	Undisturbed and subjected to drying-wetting	Thermal property test
QTU1	With free iron oxide removed and subjected to drying-wetting	Thermal property test
QTU2	With free iron oxide removed and subjected to drying-wetting	Thermal property test
MU	Undisturbed, subjected to drying-wetting and freeze-dried	MIP test
MQTU	With free iron oxide removed, subjected to drying-wetting and freeze-dried	MIP test
SU	Undisturbed, subjected to drying-wetting and freeze-dried	SEM test
SQTU	With free iron oxide removed, subjected to drying-wetting and freeze-dried	SEM test

Table 5 Repeated measurements of thermal properties of treated specimens during drying

Pre/post- water content (%)	Volumetric water content (m^3/m^3)	Thermal conductivity (W/m K)			Thermal diffusivity (mm^2/s)			Specific heat capacity (MJ/m^3 K)		
		No. 1/2/3	Mean	SD (%)	No. 1/2/3	Mean	SD (%)	No. 1/2/3	Mean	SD (%)
25.9/25.8	0.41	1.836/1.836/1.835	1.836	0.06	0.871/0.872/0.870	0.871	0.10	2.107/2.106/2.109	2.107	0.15
14.7/14.6	0.28	1.777/1.776/1.776	1.776	0.06	0.898/0.899/0.899	0.899	0.06	1.979/1.975/1.976	1.977	0.21
10.8/10.8	0.21	1.631/1.630/1.631	1.631	0.06	0.902/0.900/0.899	0.900	0.15	1.806/1.811/1.814	1.810	0.40
6.4/6.4	0.12	1.396/1.394/1.396	1.395	0.16	0.891/0.890/0.892	0.891	0.10	1.567/1.566/1.565	1.566	0.10
2.4/2.4	0.05	1.109/1.109/1.110	1.109	0.06	0.814/0.814/0.815	0.814	0.06	1.363/1.362/1.362	1.362	0.06

Pre- and post- water contents are pre- and post-measurement values of the water content during the tests, and SD is the standard deviation of the measurements

soils using the SH-1 probe, soil thermal properties could be measured.

The measurement of soil thermal properties is shown in Fig. 1c. The inner height and diameter of the specimens tested were between 5.2 and 7 cm, respectively, which matched the required dimensions of the SH-1 probe. To ensure the smooth insertion of the SH-1 probe, a dual hole for the probe was predrilled in the centre of the specimen. To ensure the test accuracy of the soil thermal properties during the air-drying and wetting processes, the SH-1 probe was always inserted into the specimens to mitigate disturbance in the samples and test positions on the accuracy in testing. In addition, the specimens were sealed with plastic bags to prevent any changes in moisture during the thermal property tests. The repeated test results of soil thermal properties are listed in Table 5, which shows that the water content of specimens was almost kept constant during the tests, and the standard deviation of the measurements was within 1%. For each specimen, the thermal properties were measured three times at 15-min intervals and the final value of each thermal property was the average value of repeated measurements.

2.4 Microstructure investigation

MIP and SEM tests were performed on certain specimens with and without the free iron oxide to investigate the microstructure evolution caused by removing free iron oxides from the soils. First, small blocks of about 0.5 cm^3 in volume were cut from the undisturbed specimens after measuring the thermal properties. The blocks were then freeze-dried and used for MIP and SEM tests. A Poremaster GT 33 (Quantachrome, Boynton Beach, FL, USA) was used for the MIP investigation. The mercury intrusion pressure of the MIP apparatus ranged from 4 to 413.7 MPa, and the corresponding entrance pore diameters ranged from 6 nm to 309.1 μm. SEM tests were conducted using the apparatus called Quanta-200.

3 Test results

3.1 Comparing thermal properties of specimens subjected to drying and wetting

Figure 2 shows the relations between thermal conductivity (TC), thermal diffusivity (TD) and specific heat capacity (SHC) of undisturbed lateritic clay with free iron oxide removed (QTU1 and QTU2) and the volumetric water content (VWC) during drying and wetting. The TC of undisturbed lateritic clays with free iron oxides removed decreased with the decrease in VWC during drying and wetting. The relations between TC and VWC existed hysteresis effects. For instance, the TC of the QTU1 specimens prepared from drying was higher than those prepared from wetting at the same VWC. Similar observations were reported by Xu et al. [37], who stated that there existed hysteresis effects on the TC of undisturbed specimens.

For undisturbed lateritic clays with removed free iron oxides, the TD first increased and then decreased with increasing VWC (Fig. 2b). The TD of undisturbed specimens with removed free iron oxides ranged from 0.728 to 0.944 mm^2/s, and a peak value of TD can be seen at a VWC of approximate 0.25 m^3/m^3. In Fig. 2c, the SHC of undisturbed specimens with removed free iron oxides changed from 1.363 to 2.476 $MJ/m^3 \bullet K$ and the values of SHC increased linearly with increasing VWC. Figure 2a–c

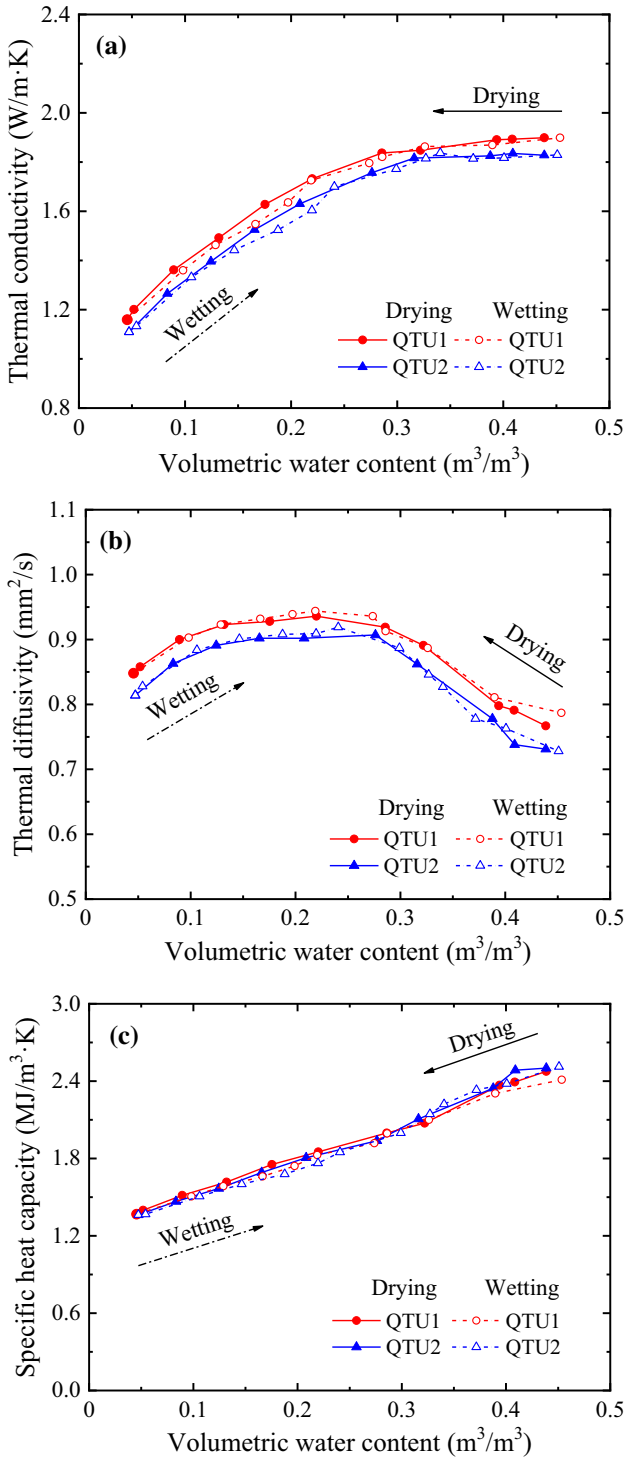

Fig. 2 Relations between the thermal properties of undisturbed specimens with free iron oxide removed (namely QTU1 and QTU2 for repeatability test) and volumetric water content during drying and wetting: **a** thermal conductivity; **b** thermal diffusivity; **c** specific heat capacity

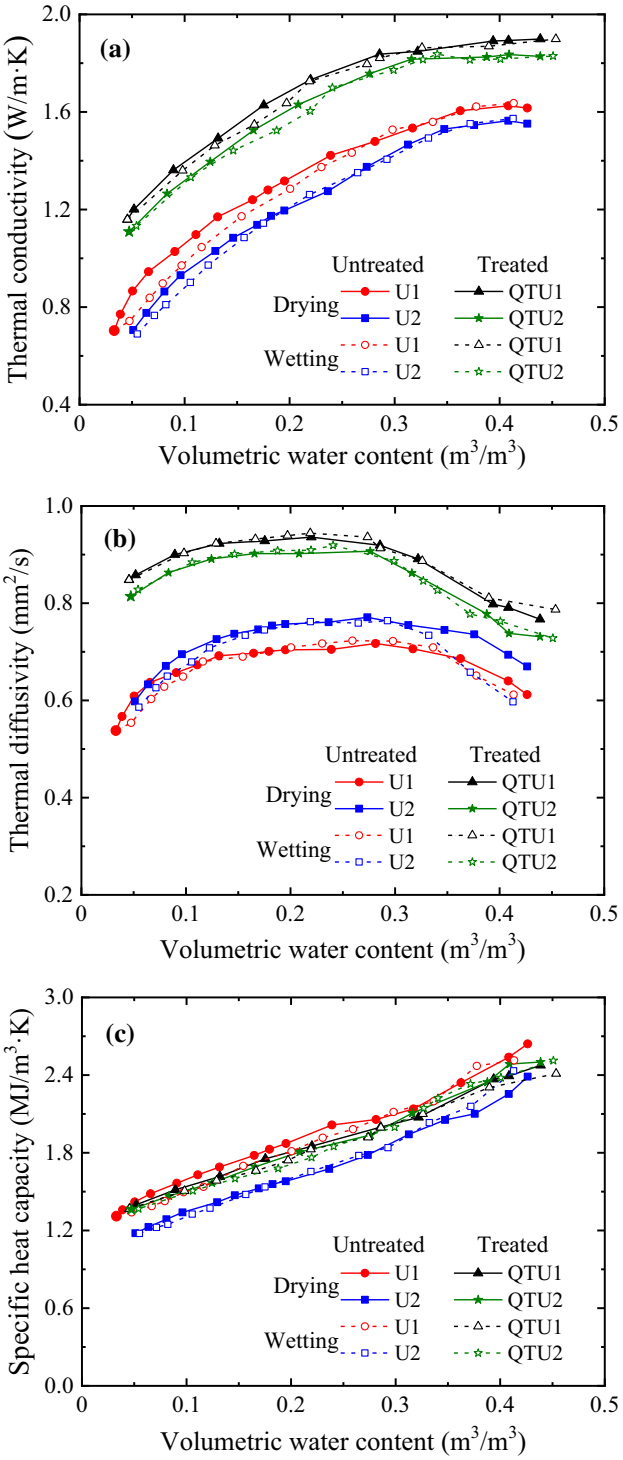

Fig. 3 Change in thermal properties of undisturbed specimens with (namely QTU1 and QTU2) and without (namely U1 and U2 for repeatability test) free iron oxide removed with volumetric water content: **a** thermal conductivity; **b** thermal diffusivity; **c** specific heat capacity

show that both the TD and SHC of undisturbed lateritic clays with removed free iron oxides did not depend on whether the water content was prepared from drying or wetting. In other words, the hysteresis effect on the TD and SHC of undisturbed lateritic clays with removed free iron oxides was not obvious.

3.2 Comparing thermal properties of specimens with and without free iron oxide removed

Figure 3 shows a comparison between the thermal properties of undisturbed lateritic clay with and without free iron during drying and wetting. The measured thermal conductivity (TC), thermal diffusivity (TD) and specific heat capacity (SHC) of undisturbed specimens are presented in Fig. 3a–c, respectively. Figure 3a shows that at the same VWC, the TC of two undisturbed specimens with removed free iron oxides (i.e., treated specimens) was higher than those containing free iron oxides (i.e., untreated specimens). With the increase in VWC from 0.03 to 0.44 m^3/m^3, the TC of two untreated specimens changed from 0.69 to 1.636 W/m K while the TC of two treated specimens ranged from 1.109 to 1.899 W/m K. On average, the TC of undisturbed specimens after removing free iron oxides was 29.3% higher than that of the specimens containing free iron oxides. In addition, the hysteresis effect on the relations between TC and VWC of undisturbed specimens was weakened after removing free iron oxides.

Test results from Fig. 3b show that the curves between TD and VWC of the treated specimens were higher than those of untreated specimens. When the VWC ranged from 0.03 to 0.44 m^3/m^3, the TDs of untreated and treated specimens (including repeatability test) ranged from 0.538 to 0.771 mm^2/s and 0.728 to 0.944 mm^2/s, respectively. The TD of the treated specimens increased by 27.7% on average compared with that of untreated specimens. As shown in Fig. 3c, the SHC of both the untreated and treated specimens increased linearly with the increase in VWC.

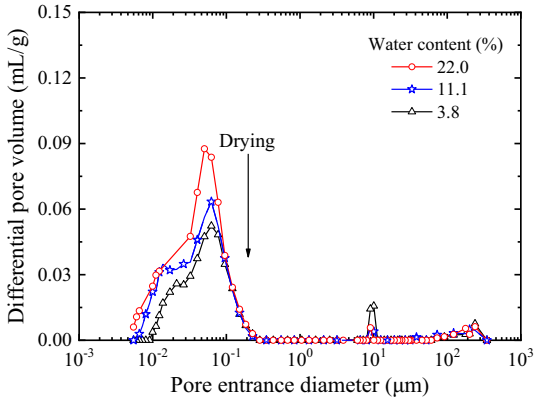

Fig. 5 The pore size distributions of undisturbed specimens with free iron oxide removed during drying

3.3 Microstructure investigation

Figure 4 compares SEM micrographs of undisturbed lateritic clays with and without free iron oxides removed at the same dry density of 1.55 g/cm^3. SEM micrographs of undisturbed specimens containing free iron oxides at magnifications of 400, 3000, and 10,000 are shown in Fig. 4a–c, respectively. Figure 4d–f show the SEM micrographs of undisturbed specimens with free iron oxide removed at magnifications of 400, 3000, and 10,000, respectively. Figure 4a and d show that after removing free iron oxides with a DCB solution, the microstructure of the undisturbed lateritic clay was denser, and certain relatively large soil pores disappeared. Moreover, before the removal of free iron oxides, the contour of the contact area between the stack bodies in the undisturbed specimens was

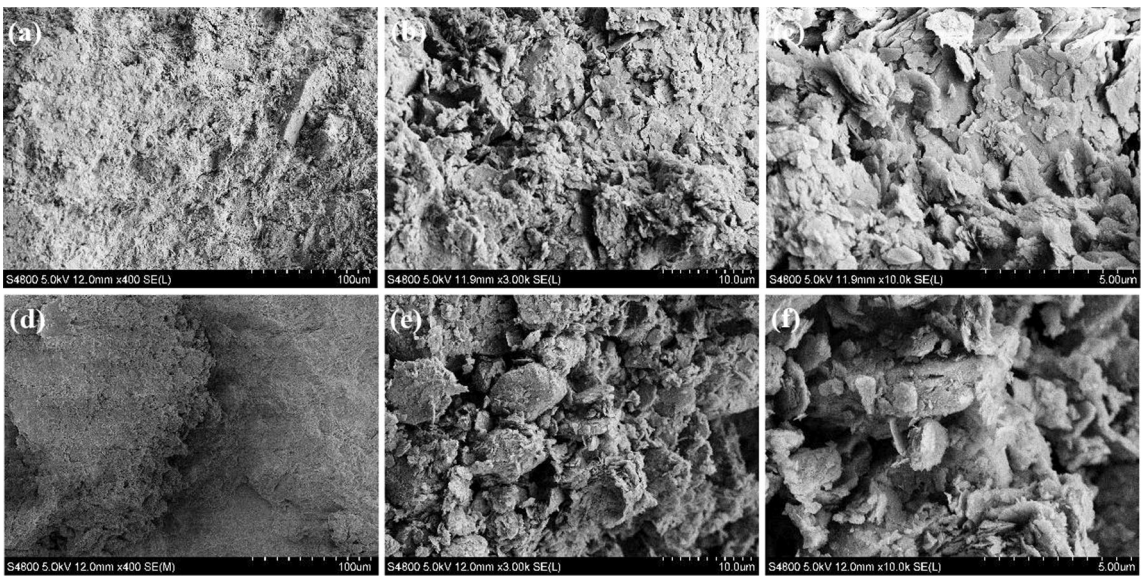

Fig. 4 SEM micrographs of undisturbed lateritic clay with and without free iron oxide removed: **a**–**c** undisturbed samples without free iron oxide removed; **d**–**f** undisturbed samples with free iron oxide removed. Magnification: **a**, **d** 400; **b**, **e** 3000; **c**, **f** 10,000

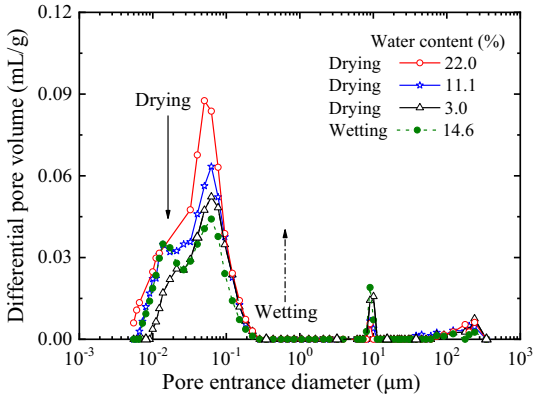

Fig. 6 The pore size distributions of undisturbed lateritic clay with free iron oxide removed during drying and wetting

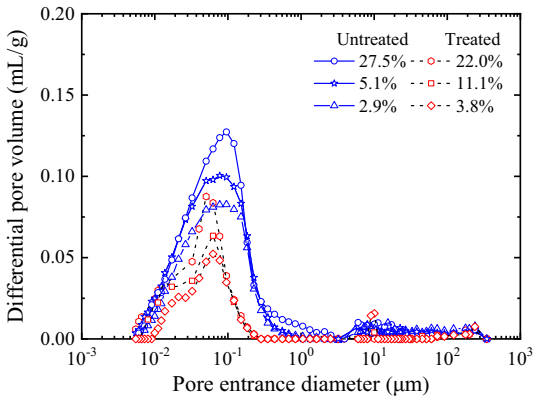

Fig. 7 The pore size distributions of undisturbed lateritic clay with and without free iron oxide removed during drying

relatively vague, which may be caused by the cementing substance. However, the debris and granular units in the microstructure of undisturbed specimens with removed free iron oxides significantly increased compared with those of untreated specimens. This may be caused by the destruction of the cementing substance after the treatment with the DCB solution.

Figure 5 shows the pore size distributions of undisturbed lateritic clays with removed free iron oxides during drying. The undisturbed lateritic clays with removed free iron oxides show a typical unimodal pore size distribution, which is mainly in the range from 0.01 to 0.1 μm. During drying, the total pore volume and number measured by MIP tests in the specimens with removed free iron oxides obviously decreased, which indicated that shrinkage deformation occurred in the specimens.

Figure 6 presents the pore size distributions for undisturbed lateritic clays with removed free iron oxides during drying and wetting. The number of soil pores increased during wetting, which showed that the specimens swelled after absorbing water. Moreover, the shrinkage of the specimens caused by pore water loss was considerably greater than the swelling of the specimens because of water absorption, which is consistent with the test results from Table 1 for the swelling and shrinkage indexes.

Figure 7 presents the pore size distributions for undisturbed lateritic clays with and without free iron oxide removed during drying. Figure 7 shows that the number of soil pores in undisturbed specimens with removed free iron oxides (i.e., treated specimens) was obviously lower than that of untreated specimens containing free iron oxides at a same initial dry density of 1.55 g/cm^3. The untreated specimens existed a few soil pores with pore size of about 10 μm (Fig. 7). However, after removing free iron oxide of the untreated specimens, these soil pores with a size of approximately 10 μm partly disappeared (Figs. 5, 6, and 7). In addition, the shrinkage of pore water loss in treated specimens was obviously larger than that in specimens containing free iron oxides.

4 Discussion

Studies by Niu et al. [18] on the soil–water retention behavior suggested that there were also a few relatively large soil pores in the undisturbed specimens, and the pore size was approximately 6 μm. After the free iron oxide was removed using selective dissolution techniques, they found that these relatively large pores disappeared, which is consistent with the test results in Figs. 4 and 7. Accordingly, they attributed the disappearance of these soil pores mainly to the removal of free iron oxides from the soil. These relatively large soil pores were formed by the bonding action of free iron oxides, which connect and wrap the soil particles in the form of bridge and cladding; thus, producing aggregates with a stable structure. Therefore, these relatively large soil pores in the specimens existed in the soil aggregates. With the removal of free iron oxides,

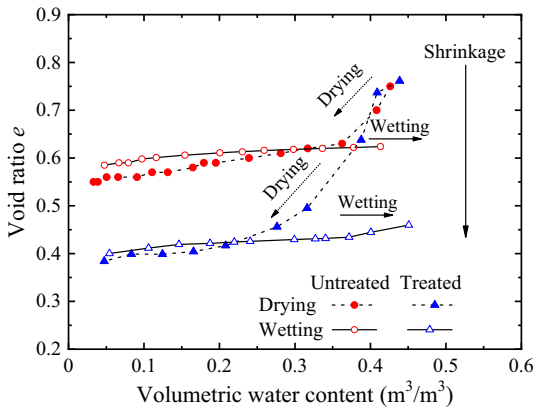

Fig. 8 Changes in void ratio of untreated and treated specimens with volumetric water content during drying and wetting

the connection and inclusion of these stable aggregates were destroyed and the internal pores disappeared. The resistance of the soil skeleton to deformation was weakened, which can explain that the shrinkage of pore water loss in the undisturbed lateritic clays with removed free iron oxides was greater than that of the untreated specimens (Fig. 7).

The results in Fig. 7 show that after the removal of free iron oxides, several soil pores with a diameter of approximately 0.1 μm in the undisturbed specimens disappeared. This is because the soil particles that make up the aggregates dispersed further after the removal of free iron oxides, which fill the adjacent pores under infiltration. As a result, some original soil pores decreased or even disappeared. Owing to the removal of free iron oxides, the ability of a soil skeleton to resist deformation is weakened, which causes an easier shrinkage of soil pores during drying. In particular, the ability of relatively large pores to resist deformation is weaker than that of small pores. Therefore, the number and size of soil pores in the specimens with removed free iron oxides were lower and smaller than those specimens containing free iron oxides (Fig. 7).

Figure 8 shows changes in the measured void ratio of untreated and treated specimens with VWC during drying and wetting. During the drying process, both the untreated and treated specimens showed obvious shrinkage deformation, particularly at high moisture levels. The specimens swelled during wetting, but the deformation caused by swelling was relatively smaller compared with that of the drying process. Moreover, obvious shrinkage deformation still existed when the specimens were first dried and then wetted to the same initial VWC. Irrecoverable shrinkage deformation occurred in this case, which agreed well with the MIP results in Fig. 6. In addition, after removing the free iron oxides from the undisturbed specimens, the shrinkage deformation caused by drying became more pronounce. This result agreed well with the MIP results in Fig. 7.

The results of the measured thermal properties of undisturbed lateritic clay with and without free iron oxides show that for the same VWC, the thermal conductivity (TC) and thermal diffusivity (TD) of the undisturbed specimens with removed free iron oxides were significantly higher than those of untreated specimens (Fig. 3). Figures 4 and 7 show that the contact between soil particles in undisturbed specimens with removed free iron oxides was more sufficient. This microstructure alteration owing to the removal of free iron oxides increased the heat transfer path between neighboring soil particles and could partly explain why the TC and TD of the treated specimens were higher than those of untreated specimens for the same VWC.

The difference in the measured TC and TD of both the treated and untreated specimens can be attributed to the different microstructures of the specimens, which affected the extent or quality of heat transfer paths through the contact points. As shown in Fig. 7, the size of the soil pores of the untreated specimens was larger than that of the treated specimens. Thus, this proved better for the connections of the clay assemblages in the treated specimens. Moreover, previous studies have shown that with increasing aggregate size, the number of relatively large pores increased, causing a decrease in the extent or quality of connections between neighboring aggregates and a reduction in the TC [12, 27]. Therefore, for a given VWC, the treated specimens possessed better transmission path for heat and thus higher TC and TD compared with those of the untreated specimens.

Hysteresis is a well-known phenomenon in many aspects of unsaturated soil behavior such as the soil–water characteristics, the capillary and effective stress, the freezing and thawing characteristics, and the process of gas hydrate growth and dissociation. Xu et al. [37] observed that the TC of both the compacted and undisturbed specimens produced by drying was higher than that by wetting. They attributed the hysteresis effects on TC mainly to the ink-bottle effect, different pore size distributions, and different volumes of entrapped air. The hysteresis effects on the TC weakened with decreasing the ink-bottle effect and increasing the uniformity of pore size distributions. The hysteresis effects on the TC of undisturbed specimens with removed free iron oxides can be seen in Fig. 3a. Unlike the untreated specimens, the hysteresis effects on the TC of treated specimens (i.e., removal of free iron oxides) were slightly weaker. As shown in Fig. 7, the pore size distributions of the treated specimens were more uniform, and most of the relatively large pores disappeared compared with the untreated specimens. This microstructural feature inevitably weakened the ink-bottle effect and effects of pore size distribution on the TC. Therefore, a stronger hysteresis effect was noticed in treated soil compared with untreated soil.

5 Conclusions

The thermal conductivity, thermal diffusivity, and specific heat capacity of both undisturbed lateritic clay with and without free iron oxides or not were measured at different VWC levels. In addition, the effects of free iron oxides and hysteresis on the soil thermal properties were investigated. A series of MIP and SEM tests were conducted on the specimens, and the effects of free iron oxides on the soil microstructure were reported. Microstructure investigations revealed the influence of hysteresis effects and free iron oxides and their mechanism on the soil thermal

properties. The following conclusions can be drawn from this study:

1. For undisturbed lateritic clays with removed free iron oxides, the thermal diffusivity of specimens prepared from drying was higher than those prepared from wetting at the same VWC. The thermal diffusivity first increased and then decreased with increasing VWC. The specific heat capacity of undisturbed specimens increased linearly with increasing VWC.
2. On average, the thermal conductivity and thermal diffusivity of undisturbed specimens increased by 29.3% and 27.7%, respectively, after removing free iron oxides. The hysteresis effect on the thermal conductivity was weakened after the removal of free iron oxides from the soil.
3. After removing free iron oxides with the DCB solution, the microstructure of the undisturbed lateritic clay was denser, and the debris and granular units significantly increased compared with those of untreated specimens. The number and size of soil pores in the specimens with removed free iron oxides (i.e., treated specimens) were lower and smaller than those of specimens containing free iron oxides (i.e., untreated specimens). The shrinkage of pore water loss in treated specimens was obviously larger than that in untreated specimens.
4. The relatively large soil pores in the undisturbed lateritic clay were formed by the bonding action of free iron oxides, which connected and wrapped the soil particles in the form of bridge and cladding, thus producing aggregates with a stable structure. After removing free iron oxides, the connection and inclusion of these stable aggregates were destroyed, which increased the heat transfer path between neighbouring soil particles. This could explain why the thermal conductivity and thermal diffusivity of treated specimens were higher than those of untreated specimens.

Acknowledgements This research was supported by the National Natural Science Foundation of China [Grant nos. 42077229, 41962014], the Natural Science Foundation of Fujian Province [Grant No. 2021J05219] and the Initial Scientific Research Fund of Young Teachers in Fujian University of Technology [Grant no. GY-Z21013].

Author contributions Yunshan Xu and De'an Sun: Conceptualization, methodology. Yunshan Xu: Data curation, writing-original draft preparation. Yunshan Xu: Visualization, investigation. Zhaotian Zeng and De'an Sun: Supervision. Yunshan Xu: Resources. Yunshan Xu and De'an Sun: Writing-reviewing and editing. Yunshan Xu and Zhaotian Zeng: Funding acquisition.

Declarations

Conflict of interest The authors declare that there are no conflicts of interest associated with publication.

References

1. Abu-Hamdeh NH, Reeder RC (2000) Soil thermal conductivity effects of density, moisture, salt concentration, and organic matter. Soil Sci Soc Am J 64(4):1285–1290. https://doi.org/10.2136/sssaj2000.6441285x
2. Ali MA, Bouazza A, Singh RM, Gates WP, Rowe RK (2016) Thermal conductivity of geosynthetic clay liners. Can Geotech J 53(9):1510–1521. https://doi.org/10.1139/cgj-2015-0585
3. Apul OG, Delgado AG, Kidd J, Alam F, Dahlen P, Westerhoff P (2016) Carbonaceous nano-additives augment microwave-enabled thermal remediation of soils containing petroleum hydrocarbons. Environ Sci Nano 3(5):997–1002. https://doi.org/10.1039/C6EN00261G
4. Bozis D, Papakostas K, Kyriakis N (2011) On the evaluation of design parameters effects on the heat transfer efficiency of energy piles. Energ Build 43(4):1020–1029. https://doi.org/10.1016/j.enbuild.2010.12.028
5. Chang TC, Yen JH (2006) On-site mercury-contaminated soils remediation by using thermal desorption technology. J Hazard Mater 128(2–3):208–217. https://doi.org/10.1016/j.jhazmat.2005.07.053
6. Cotecchia F, Chandler RJ (1997) The influence of structure on the pre-failure behaviour of a natural clay. Géotechnique 47(3):523–544. https://doi.org/10.1680/geot.1997.47.3.523
7. Duiker SW, Rhoton FE, Torrent J, Smek NE, Lal R (2003) Iron (hydr) oxide crystallinity effects on soil aggregation. Soil Sci Soc Am J 67(2):606–611. https://doi.org/10.2136/sssaj2003.6060
8. Gidigasu MD (1976) Laterite soil engineering: pedogenesis and engineering principles. Elsevier, Amsterdam
9. Han L, Ye GL, Li YH, Xia XH, Wang JH (2016) In situ monitoring of frost heave pressure during cross passage construction using ground-freezing method. Can Geotech J 53(3):530–539. https://doi.org/10.1139/cgj-2014-0486
10. He HL, Zhao Y, Dyck MF, Si BC, Jin HJ, Lv JL, Wang JX (2017) A modified normalized model for predicting effective soil thermal conductivity. Acta Geotech 12:1281–1300. https://doi.org/10.1007/s11440-017-0563-z
11. Jiang ZX, Liu LA (2011) A pretreatment method for grain size analysis of red mudstones. Sediment Geol 241(1–4):13–21. https://doi.org/10.1016/j.sedgeo.2011.09.008
12. Ju Z, Ren TS, Hu CS (2011) Soil thermal conductivity as influenced by aggregation at intermediate water contents. Soil Sci Soc Am J 75(1):26–29. https://doi.org/10.2136/sssaj2010.0050N
13. Kaune A, Turk T, Horn R (2006) Alteration of soil thermal properties by structure formation. Eur J Soil Sci 44(2):231–248. https://doi.org/10.1111/j.1365-2389.1993.tb00448.x
14. Lyu C, Sun Q, Zhang W (2020) Effects of NaCl concentration on thermal conductivity of clay with cooling. Bull Eng Geol Environ 79:1449–1459. https://doi.org/10.1007/s10064-019-01624-w
15. Li KQ, Li DQ, Chen DH, Gu SH, Liu Y (2021) A generalized model for effective thermal conductivity of soils considering porosity and mineral composition. Acta Geotech 16:3455–3466. https://doi.org/10.1007/s11440-021-01282-x
16. Liu LM, He HL, Dyck MF, Lv JL (2021) Modeling thermal conductivity of clays: a review and evaluation of 28 predictive models. Eng Geol 288(28):106107. https://doi.org/10.1016/j.enggeo.2021.106107
17. Noborio K, McInnes KJ (1993) Thermal conductivity of salt-affected soils. Soil Sci Soc Am J 57(2):329–334. https://doi.org/10.2136/sssaj1993.03615995005700020007x
18. Niu G, Sun DA, Wei CF, Shao LT (2018) Effects of free iron oxide on water retention behavior of lateritic clay. Chin J Geotech Eng 40(12):2318–2324 **(in Chinese)**

19. Ocłoń P, Bittelli M, Cisek P, Kroener E, Pilarczyk M, Taler D, Vallati A (2016) The performance analysis of a new thermal backfill material for underground power cable system. Appl Therm Eng 108:233–250. https://doi.org/10.1016/j.applthermaleng.2016.07.102
20. Ranjith PG, Zhao J, Ju MH, De Silva RVS, Rathnaweera TD, Bandara AKMS (2017) Opportunities and challenges in deep mining: a brief review. Eng Proc 3(4):546–551. https://doi.org/10.1016/J.ENG.2017.04.024
21. Raymond J (2018) Colloquium 2016: assessment of the subsurface thermal conductivity for geothermal applications. Can Geotech J 55(9):1209–1229. https://doi.org/10.1139/cgj-2017-0447
22. Rhoton FE, Römkens MJM, Bigham JM, Zobeck TM, Upchurch DR (2003) Ferrihydrite influence on infiltration, runoff, and soil loss. Soil Sci Soc Am J 67(4):1220–1226. https://doi.org/10.2136/sssaj2003.1220
23. Rowe RK (2005) Long-term performance of contaminant barrier systems. Géotechnique 55(9):631–678. https://doi.org/10.1680/geot.2005.55.9.631
24. Schwertmann U, Latham M (1986) Properties of iron oxides in some new caledonian oxisols. Geoderma 39(2):105–123. https://doi.org/10.1016/0016-7061(86)90070-4
25. Sun DA, Gao Y, Zhou AN, Sheng DC (2016) Soil–water retention curves and microstructures of undisturbed and compacted Guilin lateritic clay. Bull Eng Geol Environ 75(2):781–791. https://doi.org/10.1007/s10064-015-0765-2
26. Tang A-M, Cui YJ, Le TT (2008) A study on the thermal conductivity of compacted bentonites. Appl Clay Sci 41(3–4):181–189. https://doi.org/10.1016/j.clay.2007.11.001
27. Usowicz B, Lipiec J, Usowicz JB, Marczewski W (2013) Effects of aggregate size on soil thermal conductivity: comparison of measured and model-predicted data. Int J Heat Mass Trans 57(2):536–541. https://doi.org/10.1016/j.ijheatmasstransfer.2012.10.067
28. Wang L, Zhou AN, Xu YF, Xia XH (2022) Consolidation of partially saturated ground improved by impervious column inclusion: governing equations and semi-analytical solutions. J Rock Mech Geotech. https://doi.org/10.1016/j.jrmge.2021.09.017
29. Wilsona CA, Cloyb JM, Grahamb MC, Hamleta LE (2013) A microanalytical study of iron, aluminium and organic matter relationships in soils with contrasting hydrological regimes. Geoderma 202–203:71–81. https://doi.org/10.1016/j.geoderma.2013.03.020
30. Wiriyakitnateekul W, Suddhiprakarn A, Kheoruenromne I, Smirk MN, Gilkes RJ (2007) Iron oxides in tropical soils on various parent materials. Clay Miner 42(4):437–451. https://doi.org/10.1180/claymin.2007.042.4.02
31. Xiao Y, Ma GL, Nan B, McCartney JS (2020) Thermal conductivity of granular soil mixtures with contrasting particle shapes. J Geotech Geoenviron Eng 146(5):06020004. https://doi.org/10.1061/(ASCE)GT.1943-5606.0002243
32. Xie XT, Lu YL, Ren T, Horton R (2020) Thermal conductivity of mineral soils relates linearly to air-filled porosity. Soil Sci Soc Am J 84(1):53–56. https://doi.org/10.1002/saj2.20016
33. Xu YS, Sun DA, Zeng ZT, Lv HB (2019) Temperature dependence of apparent thermal conductivity of compacted bentonites as buffer material for high-level radioactive waste repository. Appl Clay Sci 174:10–14. https://doi.org/10.1016/j.clay.2019.03.017
34. Xu YS, Sun DA, Zeng ZT, Lv HB (2019) Effect of aging on thermal conductivity of compacted bentonites. Eng Geol 253:55–63. https://doi.org/10.1016/j.enggeo.2019.03.010
35. Xu YS, Sun DA, Zeng ZT, Lv HB (2019) Effect of temperature on thermal conductivity of lateritic clays over a wide temperature range. Int J Heat Mass Tran 138:562–570. https://doi.org/10.1016/j.ijheatmasstransfer.2019.04.077
36. Xu YS, Zhou XY, Sun DA, Zeng ZT (2022) Thermal properties of GMZ bentonite pellet mixtures subjected to different temperatures for high-level radioactive waste repository. Acta Geotech 17:981–992. https://doi.org/10.1007/s11440-021-01244-3
37. Xu YS, Zeng ZT, Sun DA, Lv HB (2020) Comparative study on thermal properties of undisturbed and compacted lateritic soils subjected to drying and wetting. Eng Geol 277:105800. https://doi.org/10.1016/j.enggeo.2020.105800
38. Yan X, Duan Z, Sun Q (2021) Influences of water and salt contents on the thermal conductivity of loess. Environ Earth Sci 80:52. https://doi.org/10.1007/s12665-020-09335-2
39. Zeng ZT, Zhao YL, Lu HB, Wei CF (2018) Experimental performance study of ground-coupled heat pump system for cooling and heating provision in karst region. Energ Build 158:971–986. https://doi.org/10.1016/j.enbuild.2017.10.071
40. Zhang XW, Kong LW, Cui XL, Yin S (2016) Occurrence characteristics of free iron oxides in soil microstructure: evidence from XRD, SEM and EDS. Bull Eng Geol Environ 75(4):1493–1503. https://doi.org/10.1007/s10064-015-0781-2
41. Zhou J, Tang YQ (2015) Centrifuge experimental study of thaw settlement characteristics of mucky clay after artificial ground freezing. Eng Geol 190:98–108. https://doi.org/10.1016/j.enggeo.2015.03.002
42. Zhou XY, He LQ, Sun DA (2022) Three-dimensional thermal modeling and dimensioning design in the nuclear waste repository. Int J Numer Anal Met 46:779–797. https://doi.org/10.1002/nag.3321

Publisher's Note Springer Nature remains neutral with regard to jurisdictional claims in published maps and institutional affiliations.